Elsevier Editorial System(tm) for Lithos
Manuscript Draft

Manuscript Number: LITHOS5197R1

Title: X-ray topographic study of a diamond from Udachnaya: implications for the genetic nature of inclusions

Article Type: Regular Article

Keywords: diamond, olivine inclusions; x-ray diffraction topography; structural defects; protogenesis; syngenesis

Corresponding Author: Dr. giovanna agrosi, Ph.D.

Corresponding Author's Institution: University "Aldo Moro"

First Author: giovanna agrosi, Ph.D.

Order of Authors: giovanna agrosi, Ph.D.; fabrizio nestola, professor; Gioacchino Tempesta, Ph.D.; marco bruno, Ph.D.; eugenio scandale, professor; Jeff W Harris, professor

Abstract: In recent years, several studies have focused on the growth conditions of the diamonds through the analysis of the mineral inclusions trapped in them. In these studies, it is crucial to distinguish between protogenetic, syngenetic and epigenetic inclusions. X-ray topography (XRDT) can be a helpful tool to verify, in a non-destructive way, the genetic nature of inclusions in diamond. With this aim, a diamond from the Udachnaya kimberlite, Siberia, was investigated. The diamond, previously studied by Nestola et al. (2011), has anomalous birefringence and the two largest olivines have typical "diamond-imposed" shapes. The study of the topographic images shows that the diamond exhibits significant deformation fields related to post growth plastic deformation. The absence of dislocations starting from the olivine inclusions, and the dark contrasts around them represent the main results obtained by XRDT, contributing to the elucidation of the relationships between the diamond and the olivines at the micron-meter scale. The dark halo surrounding the inclusions was likely caused by the effect of different thermo-elastic properties between the diamond and the inclusions. The absence of dislocations indicates that the diamond-imposed morphology did not produce the volume distortion commonly associated with the entrapment of the full-grown inclusions and, thus, only based on such evidence, a syngenetic origin could be proposed. In addition, stepped figures optically observed at the interface between diamond and one of the olivines suggest processes of selective partial dissolution that would contribute to a change in the final morphology of inclusions. These results show that a diamond morphology may be imposed to a full-grown (protogenetic) olivine during their encapsulation, suggesting that the bulk of the inclusion is protogenetic, whereas its more external regions, close to the diamond-inclusion interface, could be syngenetic.

X-ray topographic study of a diamond from Udachnaya: implications for the genetic nature of inclusions

Agrosì Giovanna [a], Nestola Fabrizio [b], Tempesta Gioacchino [a], Bruno Marco [c], Scandale Eugenio [a], Harris Jeff [d]

a) Dipartimento di Scienze della Terra e Geoambientali, Università degli Studi di Bari Aldo Moro Bari, Italia

b) Dipartimento di Geoscienze, Università di Padova, Via Giotto 1, 35121 Padova, Italia

c) Dipartimento di Scienze della Terra – Università di Torino, Via Valperga Caluso, 35, 10125 Torino, Italia -

d) School of Geographical and Earth Sciences, University of Glasgow, Glasgow G12 8QQ, UK. -

Key words: diamond, olivine inclusions; x-ray diffraction topography; structural defects; protogenesis; syngenesis

Introduction

Diamonds represent the deepest materials originating in the Earth's interior that can be found on the planet's surface. Their study has shed light on the geochemistry (both major and trace elements), geophysics, petrology, geodynamics and mineralogy of the mantle and the growth conditions of diamond, from the lithosphere to the upper/lower mantle boundary (Shirey et al., 2013 for a review; Stachel and Harris, 2008 and references therein). To obtain rigorous information about the chemical and physical conditions of diamond formation it is crucial to determine if the crystallization of the inclusions occurred before (protogenetic), during (syngenetic) or after (epigenetic) the growth of diamond. Obviously, the main information on the diamond origin is obtained when the inclusions are syngenetic because in this case the diamond and the inclusions were formed under the same physical/chemical conditions. Criteria to establish the nature of the inclusions were chiefly based on the morphology of these minerals in the diamond. Experimental evidences clearly indicate that the external shape of inclusions, whether they are monoclinic (pyroxenes), hexagonal (monosulphides), orthorhombic (olivines) or cubic (chromites or garnets), can all exhibit morphologies inside diamonds, which appear to have been imposed by their cubic diamond hosts, with the cubo-octahedral morphology being particularly common. In addition, the epitaxial relationship between inclusions and diamond host has also been investigated and has been considered to be further a strong proof of syngenesis (Bulanova, 1995; Futergendler and Frank-Kamenetsky, 1961; Harris and Gurney, 1979; Meyer, 1987; Orlov, 1977; Pearson and Shirey, 1999; Sobolev, 1977).

In contrast to the comments above, Taylor et al. (2003) argued that rare earth elements (REE) from harzburgitic garnet inclusions with apparent diamond-imposed morphologies were inconsistent with simultaneous growth with diamond and proposed a protogenetic origin for these inclusions. Recently, Bruno et al. (2014), and Nestola et al. (2014), studying crystal morphology and the crystallographic orientations of olivine inclusions with diamond-imposed morphology, also proposed that the morphology alone cannot be considered as unequivocal proof of syngenesis and that, at least for olivine from Siberia, there are not evidences of preferential epitaxial relationships with the diamond host. Consequently, the diamond formation mechanism with respect to its guest inclusions represents a topic that is still under strong debate in the scientific community.

In order to contribute to the study of the genetic nature of inclusions in diamond, the relationships between two inclusions and their host were investigated in a diamond from the Udachnaya kimberlite, Siberia. The diamond was the same sample previously studied by Nestola et al. (2011), who performed an in-situ crystal structure refinement of the inclusions to obtain data about the formation pressure. Their investigation showed that the olivine crystals had the same composition ($Fo_{92.7}$) and formed at a minimum pressure of about 5 GPa at an assumed temperature 1300°C.

In this work, we have investigated diamond using X-ray Diffraction Topography (XRDT), a non-destructive technique that makes it possible to obtain images of extended lattice defects in a mineral with a resolution limit of a few µm. This method has mainly been used to control the crystalline quality of natural and synthetic crystals used as electronic devices and to obtain information about crystalline growth mechanisms (Bowen and Tanner, 2005 and references therein). With this aim, many studies were also performed on diamonds in a non-destructive way because the low attenuation coefficient of the X-ray beam makes this mineral highly transparent to X-rays. The main results obtained on natural diamonds concerned the relationships between structural defects and the different morphologies (Moore, 2009 and references therein). However, until now this technique has rarely been used to obtain minero-petrogenetic information, and in particular there are no previous studies using topographic images to investigate the relationships between diamonds and their inclusions. In fact, samples containing inclusions were usually rejected by researchers, because complete characterization of the extended defects using X-ray topography requires crystals with a low density of structural imperfections and therefore with almost no volume defects. Nevertheless, since X-Ray Topography is sensitive to the strain associated with extended defects, the images obtained allow mapping of spatial distribution of the crystal defects in a whole sample volume. It therefore provides data for reconstruction of the crystal's growth history, even when the high density of defects prevents the high resolution of any single defect. For this reason, this type of method has recently also been used in Earth Science to provide minerogenetic information on tourmalines, garnets and beryls (Agrosì et al., 2006; Agrosì et al., 2011; Tempesta et al., 2011; Pignatelli et al., 2015). Recently, X-Ray Topography has also been successfully applied to reconstruction of the growth history of a diamond from the Finsch mine, providing a complete discrimination between growth and post-growth defects. The results obtained showed that this diamond's growth was characterized by the development of sub-individuals (twinned and untwinned) related to a relaxation phenomenon following the stress caused by the incorporation of large pyrope and orthoenstatite inclusions (Agrosì et al., 2013). These previous studies strongly suggest that this methodological approach may provide a useful and novel contribution regarding the genetic origin of inclusions in diamonds. In this paper, we show that the topographic images of the structural defects in the diamond regions surrounding the inclusions can help to explain the relationships between these volume defects and their host.

Materials and method

The diamond specimen studied in this work is colorless with longest dimension about 3 mm and has an elongate, but flattened and slightly rounded octahedral shape (Fig. 1). The sample contains three colorless olivine inclusions, (Fig. 1a); those labelled A and B were the ones previously investigated by Nestola et al. (2011). The olivine labelled C was considered not suitable by these authors for remnant pressure investigations because it was surrounded by several cracks and thus its internal pressure could be significantly released. Optical observations revealed that the diamond has anomalous birefringence (Fig. 1b) and under reflected light, etch pits as trigons were observed on the flattened (111) faces (Fig. 1c).

The diamond was investigated by XRDT, in transmission geometry with a conventional source. The technique, developed by Lang (1959), is a non-destructive imaging technique, sensitive to the strain associated with extended defects and yields spatial distribution and full characterization of the crystal defects in the crystals. This technique is used for the visualisation of defects (dislocations, twins, domain walls, inclusions, impurity distribution and so on) present in the whole sample volume. The image recorded is an integration over a spatial distribution of line sources (divergent waves) on the entrance surface of the crystal that is a distribution of monochromatic cylinder waves.

Both a vertical slit (aperture 150 μm) and a horizontal one (covering the size of the whole sample) collimated the X-rays, originated from a point source. The collimated beam was directed to the crystal specimen, which was orientated to the Bragg angle. A regulating vertical slit, next to the sample, allowed the diffracted beam to be recorded on high-resolution photographic plates and, at the same time, acted as a beam-stop for the transmitted beam. To study the whole sample, the crystal and the photographic plate were set on a platform equipped with a constant translation movement and scanned together through the X-ray beam (traverse topography). The topographs (Laue geometry) were collected using a Rigaku camera with monochromatic radiation ($MoK\alpha_1$) and with a micro-focus X-ray tube. The 1 mm thickness of the sample allows the optimum kinematical diffraction condition $\mu t \approx 1$ (μ = linear absorption coefficient; t = crystal thickness) to be made, minimizing the X-ray absorption. The resolution is about 1-2 μm. Characterization of the structural defects was performed by applying the extinction criteria to their diffraction contrasts, according to kinematical and dynamic X-ray diffraction theories (Authier and Zarka, 1994).

Results

Optical observations reveal that the two largest inclusions, labelled A and C (Fig. 2a), show a diamond-imposed morphology. Several cracks surround the C inclusion while on the upper right corner of the A inclusion small fractures can be noted as well. No discontinuity was found around the B inclusion. The stereogram shown in Figure 2b represents the crystallographic orientations of these inclusions with respect to the diamond (see Nestola et al., 2014). These orientations are different from each other and appear to be random with respect to the diamond principal axes, i.e. without any preferential epitaxial relationships. Comparisons between the optical and crystallographic observations allowed the reconstruction, in a qualitative way, of the morphology of the inclusions. Although it was not possible to measure the true angles between the faces of the olivines, it can be noted that the A and C inclusions exhibit a typical diamond-imposed morphology, whereas for the B inclusion we can only observe an elongated shape (see in Fig. 2a, the green drawings).

Additionally, optical observations, made by focusing on the surface of the A olivine inclusion reveal the piling up of laminae producing a typical stepped surface commonly due to dissolution or growth processes (Fig. 3a and b) (see Sunagawa, 2005, and references therein). We recognize two main systems of "stepped figures": the lower one in Fig. 3b resembles a triangular symmetry. The upper pattern in Fig. 3b instead shows a different symmetry, which suggests the presence of a two-fold axis. This finding is in agreement with what shown in the stereogram of Fig. 2b, where it can be observed that the direction of one of the three two-fold axes belonging to the orthorhombic symmetry of olivine A, $[00\text{-}1]_A$, is very close, almost parallel, to the[1-11] direction of diamond (Fig. 3c)**.** These observations suggest that the "stepped figures" could affect both the diamond and the olivine.

Fig. 4 presents a set of traverse topographs, which show that the whole crystal does not diffract simultaneously, because different misoriented regions of the sample are alternatively in or out of the diffraction conditions. As an example in Figs. 4a and b the images taken under the same reflection exhibit a diffraction contrast of complementary regions. In these topographs, there is a lack of diffraction contrast observed for both of the largest olivine inclusions, labelled A and C. With inclusion B the diffraction effects of the diamond lattice mask its small size and thus no further comment on this inclusion could be made.

An analysis of the diffraction contrast reveals that the diamond exhibits deformation fields affecting the entire sample. These features are believed to be due to plastic deformation (PD) taking place after the crystallization of diamond. The crystallographic direction of strain can be established applying the extinction criterion (Authier and Zarka, 1994) and this shows that, as expected, the deformation direction corresponds to that commonly found in structures with *Fd*-3*m* space group, where the energetically most favourable slip system is <110> {111}.

The main objective of this study was to investigate the relationships between the diamond matrix and the olivine crystals trapped in it, in order to shed light on the genetic nature of the inclusions. Unfortunately, the overlapping of the strain fields associated with the plastic deformation of the diamond makes the resolution of defects in the diamond regions surrounding the inclusions difficult. To minimize overlapping, three subsequent topographs were recorded under fixed exposure (Fig. 5). These topographs differ from the traverse topographs in Fig. 4, which were taken by translating the specimen and the photographic plate together. Since the image recorded on the film during translation is an integration over a spatial distribution of the divergent waves, the fixed exposure reduces the superposition of the effects caused by the beam divergence, improving the defect resolution. For this reason, the sample was repositioned under the incident beam in three successive positions (Fig. 5a) in order to obtain three different fixed topographic images, each representing different portions of diamond containing the inclusions (Fig. 5b). The topographs obtained displays more clearly the diffraction contrasts around the A and C olivines: at micron-meter scale, there is a dark contrast surrounding both inclusions and no dislocations appear to be nucleated from the olivine inclusions. The diffraction contrasts of some dislocations (D) not connected with the entrapment of the inclusions can be seen (Fig. 1c). These dislocations can be related to the trigons observed on the surfaces of sample.

Discussion

The two main results from the XRDT are (i) the presence of areas of dark contrast around the A and C olivine inclusions and (ii) absence of dislocations starting from these inclusions, which if present would appear as straight or curving lines radiating away from the inclusions. Both observations help to elucidate the relationship between diamond and the olivines.

The dark contrasts around the inclusions correspond to deformation in the diamond lattice caused by a different thermo-elastic behaviour between the olivine and the diamond host and this effect is more normally seen as birefringence haloes commonly observed around the inclusions when viewed down an optical microscope (see for example Howell, 2012, and Howell et al., 2012).

Normally, when a solid inclusion is incorporated in a full-grown state in another growing crystal, a volume defect is generated and ‘lattice closure errors’ occur by the imperfect connection between the foreign phase and the host phase that locally interrupts the crystal pattern of the diamond. The volume distortion of the crystal structure around the inclusion necessitates nucleation of a number of defects to minimize the lattice misfit. In general, nucleation of dislocations occurs to ensure a better connection between the inclusion and the host phase. In some cases, complex twinning can develop (Agrosì et al., 2013). Large inclusions usually emit bundles of many dislocations (Fig. 6). If plastic deformation occur, the grown-in dislocations will move and adopt a more or less irregular arrangement or become half-loops though still keeping anchored at the inclusions (Klapper, 200)

The lack of dislocations observed in the topographic images at the diamond/olivine interfaces is a very unusual finding. Two different scenarios can be invoked to explain the absence of defects triggered by entrapment of olivine inclusions: (i) a high lattice coherence at the diamond/olivine interfaces, i.e. the development of epitaxial relationships with a negligible misfit between the 2D lattices describing the crystal faces in direct contact. This hypothesis was recently discussed in two papers (Bruno et al., 2015; Bruno et al., 2016), which investigated four diamond/olivine interfaces at the quantum-mechanical level. (ii) Diamond and olivine are not in direct contact, but a very thin layer of amorphous matter (liquid or 2D solid) between diamond and olivine forms a more complex interface able to prevent the formation of dislocations (Bruno et al., 2016).

In our case, a definitive explanation for the absence of dislocations could only be confirmed by nanoscale investigations, in order to verify the lattice matching at the interface between diamond and olivine.

The results obtained in our study show that the diamond-imposed morphology of inclusions A and C behaves like a void in the diamond crystalline structure filled by olivine crystals that assume the morphology of diamond cavity (negative crystal shape). Then, according to the morphological criteria outlined above, it could be deduced that the A and C inclusions with their diamond-imposed morphologies are syngenetic.

The syngenetic origin involves a simultaneous growth of the inclusions and the host mineral, and implies a process under which the diamond imposes its morphology on the olivine inclusions. Previous studies proposed a process of “mutual growth” of the inclusions and diamond, during which the diamond shows a much greater “form energy”, that imposes the shape to the inclusions (Harris, 1968). The “mutual growth” presupposes a synchronous growth of inclusions and diamond and this fact has led to consider the diamond-imposed morphology as a key proof of syngenesis (Bulanova, 1995). In addition, the synchronous growth of diamond and olivine has been experimentally proved by crystallization tests of melts with peridotite-carbonatite compositions (Bobrov and Litvin, 2009; Litvin et al., 2012), even if these studies did not report diamonds with olivine inclusions.

Therefore, on the basis of the aforementioned studies and without any evidence of lattice matching at the interface, the absence of dislocations found in this work may be considered as a further proof of syngenetic origin.

With regard to the “stepped figures” here observed, it is hard to explain their origin without considering dissolution or growth processes (i.e. Sunagawa, 2005) and such processes could have played a role in the final morphology of these inclusions regardless of their syn- or protogenesis nature.

From the work of Nestola et al. (2014), it is clear that the crystallographic relationship between diamond and olivine from the Udachnaya mine is, in general, random. In addition, a more recent study by Neuser et al. (2015) using EBSD analyses from four diamonds containing eight olivines from the Yubileinaya mine, also in Yakutia, Siberia, again concluded that there was no epitaxial control during diamond and olivine formation.

Based on the aforementioned evidences, a synchronous growth of diamond and olivine inclusions is still possible because that process is not governed by epitaxy in the first place. Thus, if we take into account the possibility that the inclusions are actually protogenetic, a question to consider is under what process a full-grown protogenetic inclusion assumes a diamond-imposed morphology. Because of the lack of distinct morphology of olivine in upper mantle peridotite the potential protogenetic inclusion is probably anhedral. A further consideration is the genesis age of these diamonds and the length of time and the temperature at which they have sat in the upper mantle. In the case of Udachnaya, and assuming the inclusions are syngenetic, the genesis age of peridotitic inclusions is 2010 ± 60 Ma, the kimberlite erupted 361± 6 Ma ago and the likely temperature of formation is 1150 ± 100°C taking the average worldwide value for peridotitic inclusions in diamond, (all data from Stachel and Harris, 2008).

A shape change of a trapped inclusion in full-grown state may occur by two processes, either solid-state diffusion, or passing through resorption-recrystallization episodes.

The solid-state diffusion, comparing the physical properties of olivine and diamond, can be triggered by a different plastic behavior of olivine that eventually could undergo the morphology imposed from the diamond. This process can be favored by diffusion and /or dislocation creep along the slip systems of the olivine structure and “disclination” formation that can be detected only by means of investigations at nano-scale (Cordier et al., 2014).

Previously, Nestola et al. (2014) considered highly unlikely modification of the inclusion’s shape after encapsulation by dislocation creep mainly because such a process would request very large energies. In addition, diffusion creep process could be also ruled out because in olivine it produces crystallographic preferred orientations of grains that, in turn, involves crystallographic alignment of olivine inclusions not found in our specimen (e.g., Gung et al., 2003 and Kneller et al., 2005; Myazaki et al., 2013).

With the resorption-recrystallization scenario it is known that the natural diamond crystals brought up from the depth of the Earth passing through the region unstable for diamond have always experienced dissolution (Sunagawa, 1984 and Sunagawa et al., 1984). Indeed, the rounded morphology of the specimen and especially the trigons observed on the octahedral faces invariably testify that such process occurred rapidly during the last stage of exhumation of the diamond. Conversely, the formation of the “stepped figures” observed on the surface of inclusion A imply mechanisms of selective partial dissolution occurring during the entrapment of inclusions. This process could also explain the “imposition” of diamond morphology on the inclusions, in agreement with a previous hypothesis made by Nestola et al. (2014) for diamonds from Udachnaya. The growing diamond trapped pre-existing olivines exposed to selective dissolution, and interface diffusion processes occurred at the diamond–olivine interface, generating a diamond negative-crystal morphology.

Conclusions

This work provides new insight to solve the syngenesis-protogenesis debate through the analyses of structural defects.Two main results were obtained: 1) absence of dislocations nucleated from the olivine inclusions at the interface with diamond and 2) presence of “stepped figures” observed on the surface of the bigger inclusion again at the interface with diamond.

The above results 1) and 2) can be considered consistent with a “syngenetic interface” between diamond and olivine as the absence of dislocations at the interface can be justified only by a perfect lattice matching between the two phases. Furthermore, the stepped figures suggest a simultaneous growth through a resorption-recrystallization process, even if these figures would provide an indication of syngenesis only for the outer layers close to the interface between diamond and olivine but not for the larger volume of the inclusion.

However, to demonstrate definitely the perfect lattice matching at interface between diamond and olivine, images of interface at near atomic scale, not yet available in literature, would be necessary.

Finally, although our results provide information never reported before for the diamond-olivine pair, the strong debate between syngenesis and protogenesis still remains controversial and requires further information on such complex growth system.

Acknowledgements

The authors are very grateful to the Editor Prof. M. Scambelluri, to the reviewer dr. Anthony Burnham, and to the anonymous reviewer for their constructive comments and suggestions that allowed appreciable improvement of the manuscript. The research was supported by ERC Starting Grant INDIMEDIA (grant number 307322) awarded to Fabrizio Nestola, University of Padova (Italy).

References

Agrosì, G., Bosi, F., Lucchesi, S., Melchiorre, G., Scandale, E., 2006. Mn-tourmaline crystals from island of Elba (Italy): growth history and growth marks. American Mineralogist 91, 944-952.

Agrosì, G., Scandale, E., Tempesta, G., 2011. Growth marks of titanian-andradite crystals from Colli Albani (Italy). Periodico Di Mineralogia 80, 89–104.

Agrosì, G., Tempesta, G., Scandale, E., Harris, J.W., 2013. Growth and post-growth defects of a diamond from Finsch mine (South Africa). European Journal of Mineralogy 25 (4), 551-559.

Authier, A. and Zarka, A., 1994. X-ray topographic study of the real structure of minerals, in A.S. Marfunin (Ed.), Composition, Structure and Properties of Mineral Matter. Springer -Verlag, Berlin, pp. 221-233.

Bowen D.K. and Tanner B.K., 2005. High Resolution X-Ray Diffractometry and Topography, CRC Press (Ed.), pp. 252.

Bobrov, A.V., and Litvin, Y.A., 2009. Peridotite–eclogite–carbonatite systems at 7.0–8.5 GPa: Concentration barrier of diamond nucleation and syngenesis of its silicate and carbonate inclusions. Russian Geology and Geophysics 50, 1221– 1233. doi:10.1016/j.rgg.2009.11.020.

Bruno, M., Massaro, F.R., Prencipe, M., Demichelis, R., La Pierre, M., Nestola, F., 2014. Ab Initio Calculations of the Main Crystal Surfaces of Forsterite (Mg_2SiO_4): A Preliminary Study to Understand the Nature of Geochemical Processes at the Olivine Interface. Journal of Physical Chemistry C 118, 2498-2506.

Bruno, M., Rubbo, M., Pastero, L., Massaro, F.R., Nestola, F., Aquilano, D., 2015. Computational approach to the study of epitaxy: natural occurrence in diamond/olivine and aragonite/zabuyelite. Crystal Growth Design 15, 2979–2987.

Bruno M., Rubbo M., Aquilano D., Massaro F. R., Nestola F., 2016. Diamond and its olivine inclusions: a strange relation revealed by ab initio simulations. Earth & Planetary Science Letters 435, 31-35.

Bulanova, G.P., 1995. The formation of diamond. Journal of Geochemical Exploration 53, 1–23. doi:10.1016/0375-6742(94)00016-5.

Cordier, P., Demouchy, S., Beausir, B., Taupin, V., Barou, F., Fressengeas, C., 2014. Disclinations provide the missing mechanism for deforming olivine-rich rocks in the mantle. Nature 507, 51-56.

Diehl R., Herres N., 2004. X-ray fingerprinting routine for cut diamonds. Gems & Gemology, 40/1, 40–57.

Futergendler, S.I., and Frank-Kamenetsky, V.A., 1961. Oriented inclusions of olivine, garnet and chrome-spinel in diamonds: Zapisky Vsesoyuznogo Mineralogicheskogo Obshestva 90, 230–236. [In Russian].

Gung, Y., Panning, M., and Romanowicz, B., 2003. Global anisotropy and the thickness of continents. Nature 422, 707–711.

Harris, J.W., 1968. The recognition of diamond inclusions. Pt. 1: Syngenetic inclusions. Industrial Diamond Reviews 28, 402–410.

Harris, J.W., and Gurney, J.J., 1979. Inclusions in diamond, in: Field, J.E., (Ed.), Properties of diamond. Academic Press, London, pp. 555–591.

Howell, D., 2012. Strain-induced birefringence in natural diamond: a review. European Journal of Mineralogy 24, 575–585.

Howell, D., Wood, I.G., Nestola, F., Nimis, P., and Nasdala, L., 2012. Inclusions under remnant pressure in diamond: a multi-technique approach. European Journal of Mineralogy 24, 563-573, doi: 10.1127/0935-1221/2012/0024-2183.

Klapper H., 2000. Generation and propagation of dislocations during crystal growth. Materials Chemistry and Physics 66, 101–109.

Kneller, E.A., van Keken, P.E., Karato, S.-I., and Park, J., 2005. B-type olivine fabric in the mantle wedge: insights from high-resolution non-Newtonian subduction zone models. Earth and Planetary Science Letters 237, 781–797.

Lang, A.R., 1959. The projection topograph: a new method in X-ray diffraction microradiography. Acta Crystallographica 12, 249-250.

Litvin, Y.A., Vasil'ev, P.G., Bobrov, A.V., Okoemova, V.Y., and Kuzyura, A.V., 2012. Parental media of natural diamonds and primary mineral inclusions in them: Evidence from physicochemical experiment. Geochemistry International 50, 726–759. doi:10.1134/S0016702912070051.

Meyer, H.O.A., 1987. Inclusions in diamond, in: Nixon, P.H. (Ed.), Mantle xenoliths. John Wiley & Sons, Chichester, pp. 501– 522.

Moore M., 2009. Imaging diamond with x-rays. Journal of Physiscs: Condensed Matter 21, 364217, pp. 15. doi:10.1088/0953-8984/21/36/364217

Myazaki, T., Sueyoshi, K., Hiraga, T., 2013. Olivine crystals align during diffusion creep of Earth's upper mantle. Nature 5012, 321-326.

Neuser, R.D., Shertl, H.P., Logvinova, A.M., Sobolev, N.V., 2015. An EBSD study of olivine inclusions in Siberian diamonds: evidence for syngenetic growth?. Russian Geology and Geophysics 56, 321-329.

Nestola, F., Nimis, P., Angel, R.J., Milani, S., Bruno, M., Prencipe, M., Harris, J.W., 2014. Olivine with diamond-imposed morphology included in diamonds. Syngenesis or protogenesis?. International Geology Review 56 (13), 1658-1667. doi: 10.1080/00206814.2014.956153

Nestola, F., Nimis, P., Ziberna, L., Longo, M., Marzoli, A., Harris, J.W., Manghnani, M.H., and Fedortchouk, Y., 2011. First crystal-structure determination of olivine in diamond: Composition and implications for provenance in the Earth's mantle. Earth and Planetary Science Letters 305, 249– 255. doi:10.1016/j.epsl.2011.03.007

Orlov, Y.L., 1977. The mineralogy of the diamond. John Wiley & Sons, New York [Translation of Mineralogiiaalmaza, Izdatel'stvaNauka, 1973, in Russian].

Pearson, D.G., and Shirey, S.B., 1999. Isotopic dating of diamonds, in: Lambert, D.D., Ruiz, J., (Eds.), Application of radiogenic isotopes to ore deposit research and exploration. Society of Economic Geologists, Boulder, Colorado, pp. 143–171.

Pignatelli I., Giuliani G., Ohnenstetter D., Agrosì G., Mathieu S., Morlot C., Branquet Y., 2015. Colombian trapiche emeralds: recent advances in understanding their formation. Gems and Gemology 51 (3) 222-259. doi:10.5741/GEMS.51.3.222.

Shirey, S.B., Cartigny, P., Frost, D.J., Keshav, S., Nestola, F., Nimis, P., Pearson, D.G.,Sobolev, N.V., Walter, M.J., 2013. Diamonds and the geology of mantle carbon, in: Hazen, R.M., Jones, A.P., and Baross, J.A., (Eds.), Carbon in Earth: Reviews in Mineralogy & Geochemistry 75, pp. 335-421.

Sobolev, N.V., 1977. Deep-seated inclusions in kimberlites and the problem of the composition of the upper mantle, American Geophysical Union, Washington, D.C.,

Stachel, T., and Harris, J.W., 2008. The origin of cratonic diamonds – Constraints from mineral inclusions. Ore Geology Reviews 34, 5–32. doi:10.1016/j.oregeorev.2007.05.002

Sunagawa, I., 2005. Crystals: Growth, Morphology and Perfection: Cambridge University Press.

Sunagawa, I., Tsukamoto, K., Yasuda, T., 1984. Surface microtopographic and X-ray topographic study of octahedral crystals of natural diamond from Siberia. in: Sunagawa I. (ed.), Materials Science of the Earth's Interior. Terra Science publications, Tokyo/D Reidel, Dordrecht, pp. 331-349.

Sunagawa, I., 1984, Morphology of natural and synthetic diamond crystals. In: Sunagawa, I., (ed.), Materials of the Earth's interior. Terra Scientific Publishing Company, Tokyo, pp. 303–330.

Taylor, L.A., Anand, M., and Promprated, P., 2003. Diamonds and their inclusions: Are the criteria for syngenesis valid? In: Eighth International Kimberlite Conference, Long Abstract Volume, Victoria, Canada.

Tempesta, G., Scandale, E., Agrosì, G., 2011. Striations and hollow channels in rounded beryl crystals. Periodico di Mineralogia 79/1, 75-87.

Wierzchowski W. K., Moore M., Makepeace A. P. W., Yacoot A., 1991. X-ray topographic studies and measurement of lattice parameter differences within synthetic diamonds grown by the reconstitution technique. Journal of Crystal Growth 114, 209–27.

Figure captions

Figure 1. Optical micrographs of sample. a) Transmitted light under parallel nicols. Note three colorless inclusions of olivine previously studied by Nestola et al. (2011), named A, B and C. b) Transmitted light under crossed nicols. Note the anomalous birefringence of diamond. c) Optical micrograph of sample under reflected light. Note the rounded cubo-octahedral morphology with two flattened parallel {111} faces showing trigons.

Figure 2. a) Optical micrograph of inclusions with the corresponding schematic drawings (in green) of the reconstructed morphology: the A and C inclusions show a very typical diamond-imposed morphology. b) Stereogram obtained by XRD data showing the relative crystallographic orientations of the olivine inclusions, labelled A and B, and their diamond host (modified from Nestola et al. 2014).

Figure 3. a) Optical micrograph taken under reflecting light, focusing the surface of inclusion A; b) enlargement of the surface of the inclusion A: note “stepped” figures; c) schematic sketch showing the features associated to the 2-fold and 3-fold symmetry axes.

Figure 4. X-Ray traverse topographs taken using $MoK\alpha_1$ radiation. Arrows show the diffraction vector projection **g**. a) and b) **g**=02-2; c) **g**=-311; d) **g**= 1 -1 1.The topographic images show only the lack of contrast corresponding to inclusions A and C, whereas the inclusion B is not detectable because of its limited size. PD: plastic post growth deformation. Projection effects of the asymmetric reflections give the difference between the size of sample and the size of the different topographic images.

Figure 5. a) optical images showing three regions on which the X-Ray topographs under fixed exposure were taken. b) X-Ray topographs under fixed exposure with the same diffraction vector **g**=-311 (see the small arrow). The topographic images correspond to the three successive positions of the sample under the beam (see the big arrows). A and C represent the olivine inclusions, D represents the dislocations subtending the trigons observed on the diamond surface. Dark contrasts surround the inclusions. No dislocations nucleated from the olivine inclusions are observed.

Figure 6. X-ray traverse topographs taken with $MoK\alpha_1$ radiation revealing examples of dislocations nucleated from inclusions. a) Synthetic diamond with a number of fans of dislocations (D) nucleated from small inclusions (I), (**g**=111) (modified from Wierzchowski et al. 1991). b) Natural octahedral diamond with bundles of dislocations (D) radiating away from a large inclusion (I) , (**g**= 220) (modified from Diehl and Herres 2004).

Figure1

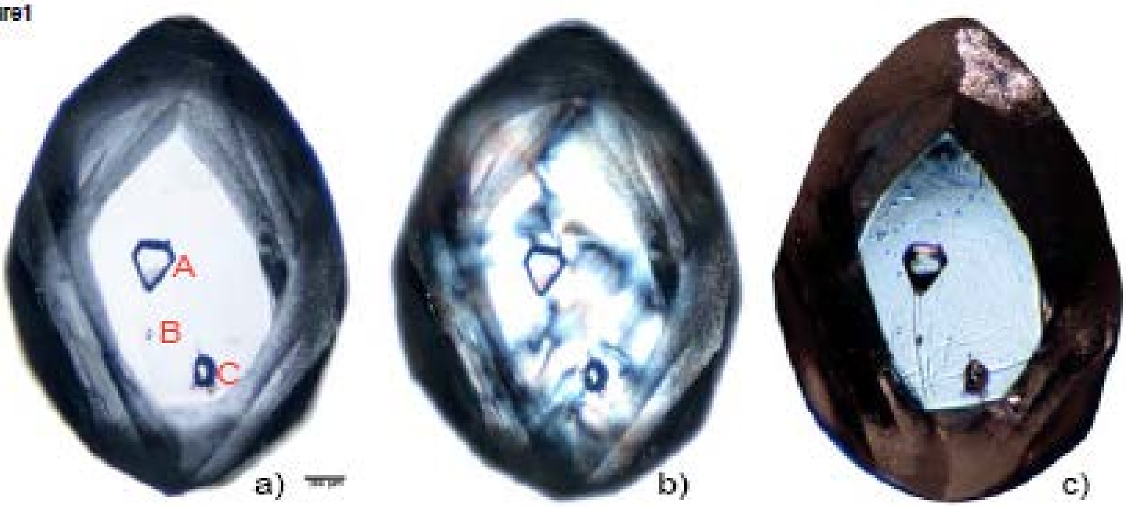

448

Figure2
Click here to download high resolution image

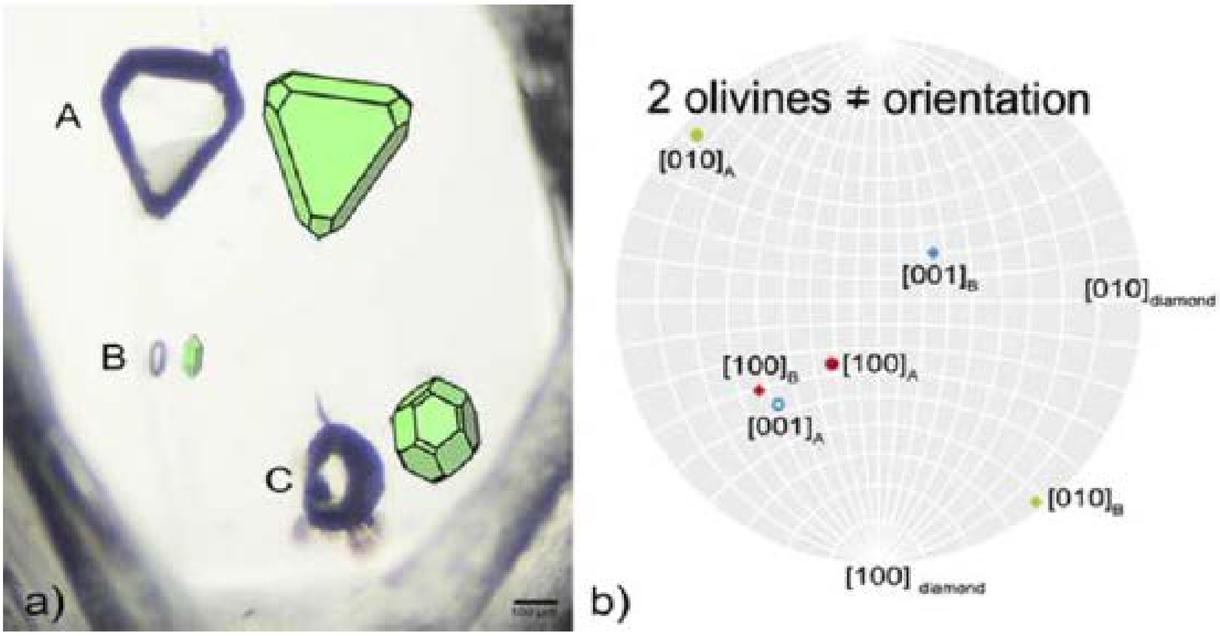

Figure3
Click here to download high resolution image

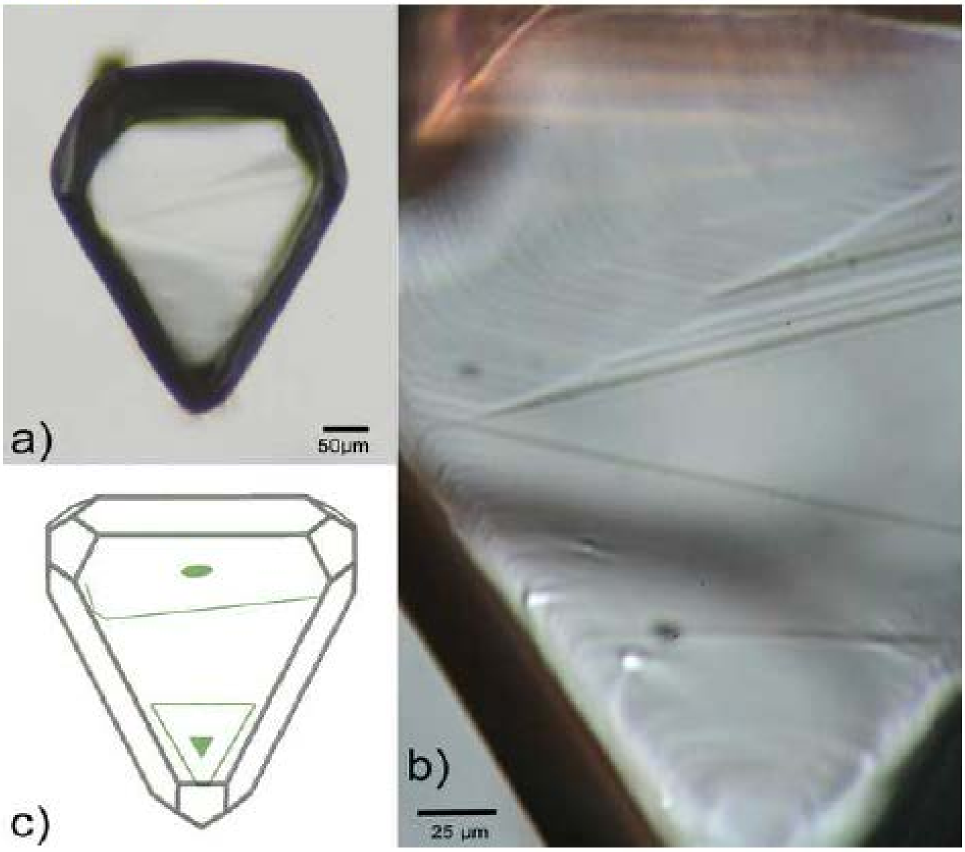

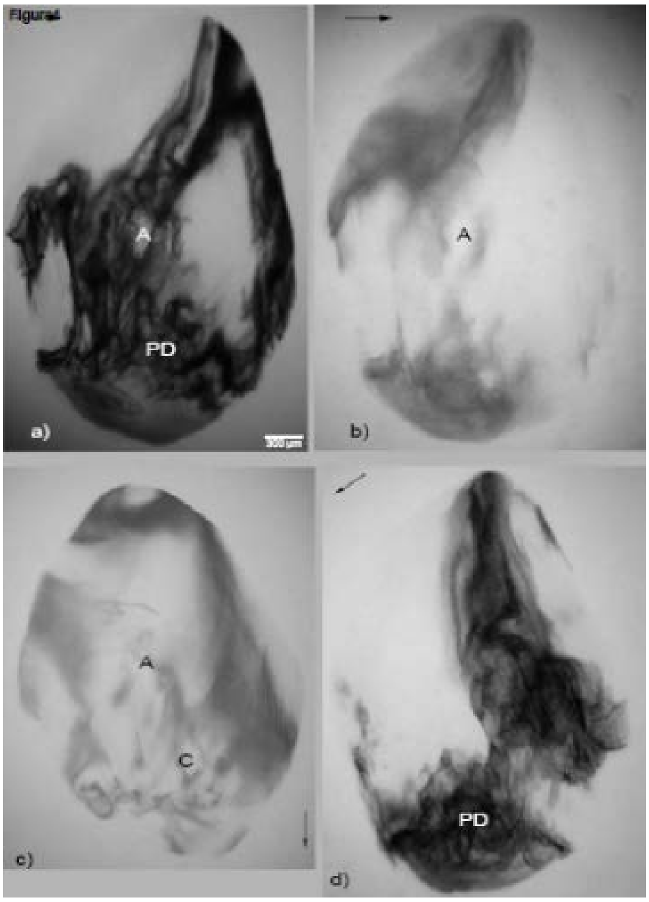

449

Figure 5
Click here to download high resolution image

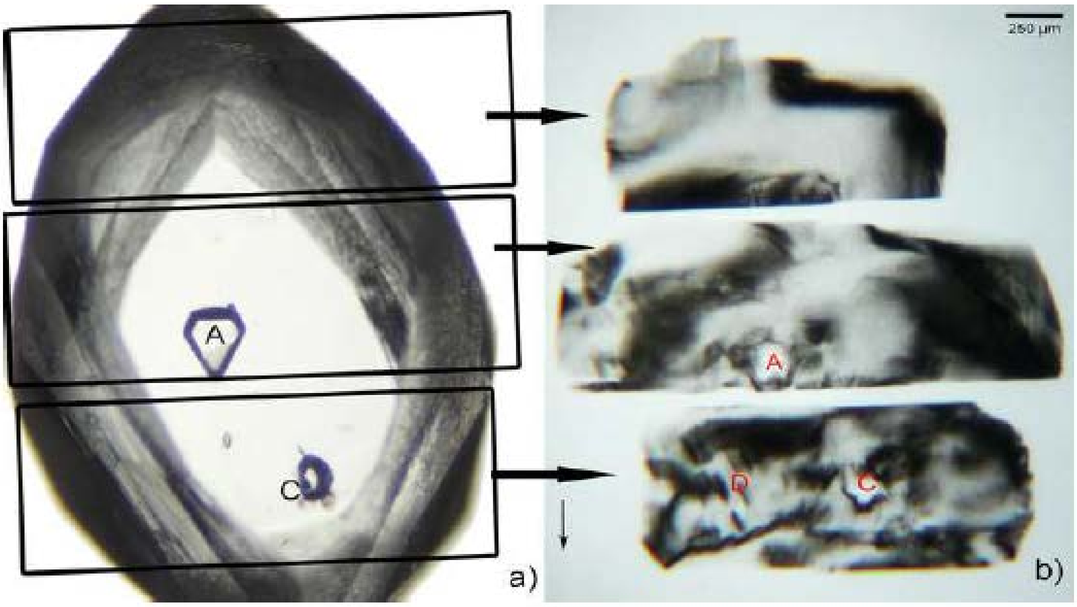

Figure 6
Click here to download high resolution image